# Dynamic Superior Capsular Reconstruction for Irreparable Massive Rotator Cuff Tears

## Histologic Analysis in a Rat Model and Short-term Clinical Evaluation

Huaisheng Li,* MS, Yatao Liao,* MS, Baoyong Jin,* MS, Mingyu Yang,* PhD, Kanglai Tang,* MD, PhD, and Binghua Zhou,*† MD, PhD
*Investigation performed at Southwest Hospital, Army Medical University, Chongqing, China*

**Background:** Superior capsular reconstruction (SCR) has been demonstrated to be a valuable treatment for patients with irreparable massive rotator cuff tears (IMRCTs). However, the torn medial supraspinatus (SSP) tendons, which acted as dynamic stabilizers, were left untreated in conventional SCR, and the dynamic force from the SSP tendon was not restored.

**Purpose:** To evaluate the effect of dynamic SCR (dSCR) on fascia-to-bone healing in a rat model, and to compare the short-term clinical effectiveness of dSCR and SCR using autologous fascia lata (FL) in patients with IMRCTs.

**Study Design:** Controlled laboratory study and cohort study; Level of evidence, 3.

**Methods:** A total of 50 rats were divided randomly into 2 groups: the dSCR group and the SCR group (25 rats per group). First, chronic IMRCTs were created, and then the torn tendons in both groups were subjected to SCR using autologous thoracolumbar fascial (TLF) grafts. The remnant of the SSP tendon was sutured to the medial part of the TLF graft in the dSCR group but not in the SCR group. Histologic sections were assessed at 1, 2, 4, 8, and 16 weeks postoperatively. In the clinical study, 22 patients (9 SCR, 13 dSCR) were analyzed. The recovery of shoulder function, including the active range of motion (ROM), visual analog scale (VAS), American Shoulder and Elbow Surgeons score, Constant score, and University of California Los Angeles score, acromiohumeral distance (AHD), and fatty infiltration, was evaluated before surgery and at the last follow-up.

**Results:** Histologic analysis of the fascia-to-bone junction in the rat model showed that the TLF gradually migrated into tendon-like tissue over the rotator cuff defects in both groups, and the modified tendon maturation score of the fascia-to-bone interface in the dSCR group was higher than that in the SCR group at 4 weeks (12.20 ± 1.30 vs 14.60 ± 1.52; $P = .004$), 8 weeks (19.60 ± 1.14 vs 22.20 ± 1.10; $P = .019$), and 16 weeks (23.80 ± 0.84 vs 26.20 ± 0.84 $P = .024$). The dSCR group showed earlier fibrocartilage cell formation and angiogenesis. In the clinical study, all 22 patients completed a minimum of 12 months of follow-up after surgery, and the mean follow-up duration was 22.89 ± 7.59 months in the SCR group and 25.62 ± 7.32 months in the dSCR group. The patients in both groups showed significant improvements in terms of ROM, shoulder function scores, and AHD. At the last follow-up, abduction (56.67° ± 27.39° vs 86.54° ± 30.37°; $P = .029$), external rotation (25.00° ± 9.35° vs 33.08° ± 8.55°; $P = .049$), internal rotation cone rank (–2.78 ± 2.44 vs –4.38 ± 1.12; $P = .049$), VAS (–3.00 ± 0.87 vs –3.92 ± 0.95; $P = .031$) and Constant (47.89 ± 15.39 vs 59.15 ± 9.74; $P = .048$) scores, and the AHD improvement degree (3.06 ± 1.41 mm vs 4.38 ± 1.35 mm; $P = .039$) in the dSCR group were significantly improved compared with those in the SCR group. The results of fatty infiltration at the last follow-up showed that there was significant improvement compared with the preoperative results in both the conventional SCR ($P = .036$) and the dSCR ($P = .001$) groups. However, there were no significant differences between the 2 groups ($P = .511$).

**Conclusion:** dSCR can promote faster fascia-to-bone healing in a rat model, and the dSCR technique could provide a preferable treatment option for patients with IMRCTs.

**Clinical Relevance:** dSCR might restore the dynamic of SSP in some sense and then improve the fatty infiltration in the SSP.

**Keywords:** fascia-to-bone healing; irreparable massive rotator cuff tear; superior capsular reconstruction; dynamic; clinical outcome

The American Journal of Sports Medicine
2023;51(5):1255–1266
DOI: 10.1177/03635465231156619


Massive rotator cuff tears (MRCTs) have been defined as tears ≥5 mm and/or tears involving ≥2 tendons.[15,44] When the footprint of the rotator cuff cannot be reconstructed under appropriate tension, it is termed an

irreparable MRCT (IMRCT).[30,36] Severe shoulder dysfunction and RCT arthropathy could be caused by IMRCTs losing superior stability.[9] The nonoperative treatments for IMRCTs include changing the activity level, nonsteroidal anti-inflammatory drugs, corticosteroid injection, and physical therapy,[51] and the surgical treatments for IMRCTs can be classified as joint arthroplasty and joint-preserving treatment, which include soft tissue reconstruction, tendon transfer, and palliative treatment.[4,6,35,36,50-53] There is no consensus for the surgical treatment of IMRCTs, and the different treatments have their indications.

Superior capsular reconstruction (SCR), first described by Mihata et al in 2013, substitutes a graft between the superior glenoid and the humeral head.[38-40] Different grafts, such as the fascia lata (FL), long head of the biceps tendon (LHBT), acellular dermal allograft, xenograft, or synthetic graft, have been used and showed significant clinical improvement.[7,8,26] SCR restores the stability of the glenohumeral joint and improves the function of the shoulder joint.[29,34] Anatomic supraspinatus (SSP) tendons can dynamically stabilize the shoulder and assist the deltoid muscle in abducting the shoulder joint.[7] However, conventional SCR does not restore the anatomy of the SSP, and incomplete dynamic function recovery after SCR still exists.

Restoring the dynamics of remnant SSP tendons could maximize clinical outcomes when performing SCR.[3] However, injured insertions did not regenerate the grade tissue.[45] Moreover, chronic degenerative changes in rotator cuff muscles, tendons, and bone were not reversible and led to inferior healing characteristics after repair.[24] Biologic augmentation of degenerative tissue has the potential to enhance biomechanical and histologic integrity.[27] Fascial autografts have been confirmed to achieve good fascia-to-bone healing.[32] The revascularization of the FL in the SCR mainly comes from the fascia-to-bone interface.[33] The bridging technique between the graft and medial remnant tendon could restore the dynamics of the SSP but has a high retear risk.[22] To minimize the retear rate and enhance fascia-to-tendon healing, the dynamic SCR (dSCR) technique involves suturing the medial remnant of the SSP tendons to the FL graft directly after conventional SCR, and revascularization of the fascia-to-tendon interface will come from both the fascia-to-bone interface and SSP muscle and tendon. In addition, mechanical stretch could induce the differentiation of stem cells and enhance tendon-to-bone healing.[56] However, the effect of the dynamic function of the remnant SSP tendon on fascia-to-bone healing is still unclear. Additionally, whether the dynamic reduced function recovers after dSCR requires further study.

Here, we established dSCR and SCR rat models with MRCT using thoracolumbar fascia (TLF) and histologically investigated the effects of dSCR on fascia-to-bone healing. In clinical research, we described the dSCR technique with SSP tendon remnant suturing to the FL autograft and documented short-term clinical outcomes in patients with IMRCTs. We hypothesized that dSCR would have a faster histologic healing process on the fascia-to-bone interface than SCR in the rat model, and dSCR can be a preferable clinical choice for patients with IMRCTs by restoring dynamic function.

## METHODS

For the animal experiment, fifty 16-week-old male Sprague-Dawley rats were used, as approved by our animal welfare and ethics committee (No. AMU-WEC20191870). All rats were first treated to create the chronic IMRCT models and were then divided randomly into 2 groups (25 rats per group): the dSCR group and the SCR group. The rats from both groups were sacrificed for samples at 1, 2, 4, 8, and 16 weeks postoperatively (n = 5 each group at the time point), and then those samples were used for gross examination and histologic analysis. For the clinical research, 22 patients who underwent dSCR or SCR were analyzed, and this research was approved by our ethics committee (No. KY2020128). The improvement in shoulder function scores and the active range of motion (ROM) were recorded. Meanwhile, radiographs and magnetic resonance imaging (MRI) scans were used to evaluate the change in the acromiohumeral distance (AHD) and fatty infiltration of the SSP muscle, respectively. Figure 1 shows the study design.

### Animal Study

#### *Animal Model Preparation*

A rat with chronic MRCT based on previous studies was used.[18,32] First, we created chronic massive rotator cuff defects in the SSP tendons in the right forelimbs of all 50 rats. Rats were anesthetized with 1% sodium pentobarbital (40 mg/kg intraperitoneally), and the right forelimb and the back were shaved and washed with 2% chlorhexidine and 70% ethanol. Later, an approximately 2-cm longitudinal incision was centered over the glenohumeral joint, extending proximally along the belly of the SSP and distally along the shaft of the humerus. The middle belly of the deltoid was separated bluntly down to the lateral aspect of the proximal humeral shaft. The

†Address correspondence to Binghua Zhou, MD, PhD, Department of Sports Medicine, Southwest Hospital, Army Medical University, No. 30 Gaotanyan Main Street, Chongqing, 400038, China (email: yijian510868@hotmail.com).

*Department of Sports Medicine, Southwest Hospital, Army Medical University, Chongqing, China.

H.L. and Y.L. contributed equally to this work.

Submitted October 6, 2022; accepted December 30, 2022.

One or more of the authors has declared the following potential conflict of interest or source of funding: This study is supported by Chongqing Yingcai Projects for Creative Leading Talents (CQYC20200303135). AOSSM checks author disclosures against the Open Payments Database (OPD). AOSSM has not conducted an independent investigation on the OPD and disclaims any liability or responsibility relating thereto.

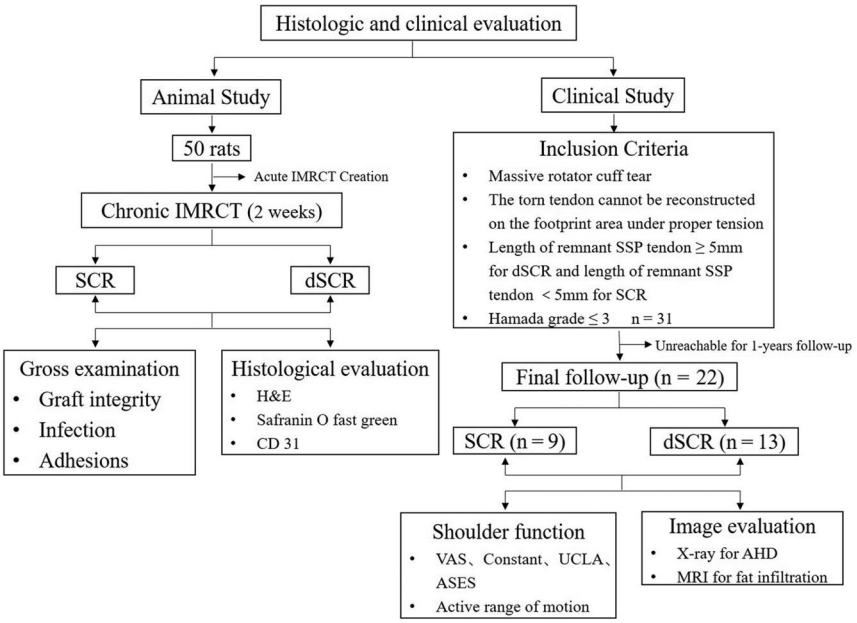


**Figure 1.** Overall study design. AHD, acromiohumeral distance; ASES, American Shoulder and Elbow Surgeons; dSCR, dynamic superior capsular reconstruction; H&E, hematoxylin and eosin; IMRCT, irreparable massive rotator cuff tear; MRI, magnetic resonance imaging; SCR, superior capsular reconstruction; SSP, supraspinatus; UCLA, University of California Los Angeles; VAS, visual analog scale.

acromioclavicular joint was incised. The SSP tendon was identified and detached from its insertion on the proximal humerus. In the SCR group, the whole SSP tendon, approximately 5 to 6 mm in length, was removed from the underlying capsule using scissors. In the dSCR group, a 2-mm remnant of the SSP tendon in the medial region remained and was rolled up to make 2 sutures to prevent spontaneous retraction and healing with surrounding tissue, followed by routine incision closure.[55]

Two weeks after the first surgery, a vertical skin incision was made over the back beside the lumbar spine, and a section of TLF 2 times the size of the torn SSP tendon, approximately 5 × 12 mm, was harvested (Figure 2B). Then, the TLF autograft was placed in phosphate-buffered saline solution for later use, and the back incision was sutured layer by layer. For the right forelimbs, the skin and deltoid were sequentially split along the previous incision, and the scar tissue and tagged sutures were removed to expose the SSP defect. Later, the greater tuberosity and superior glenoid were refreshed; one end of the TLF was fixed onto the great tuberosity through cross-shaped bone tunnels, and the other end was fixed onto the superior glenoid through the holes that were punched by needles (Figure 2, F-H). In the dSCR group, the remnant of the SSP tendon was sutured to the medial part of the TLF (Figure 2, I and J); the SCR group did not receive this treatment. The wound was closed using 4-0 Proline (Ethicon, Shanghai, China). After closure, the rats were allowed unrestricted cage mobility.

### *Gross Examination*

The rats in each group were euthanized by carbon dioxide inhalation at weeks 1, 2, 4, 8, or 16 postoperatively; the macroscopic examination criteria included graft integrity, signs of infection, and adhesions to represent the healing process.[20]

### *Histologic Analysis*

After the macroscopic evaluation of fascia-to-bone healing, the fascia-to-bone junction samples were fixed in 4% paraformaldehyde (pH, 7.5) for 48 hours, decalcified in 20% formic acid for 72 hours, and then embedded in paraffin. Sections (thickness, 5 μm) were cut in the sagittal plane and stained with hematoxylin and eosin (H&E) and safranin O fast green for histologic analysis. The histologic findings were semiquantitatively evaluated by the modified tendon maturation score.[20,32] The cartilage staining areas were assessed by using ImageJ software (National Institutes of Health).

### *Immunohistochemical Analysis*

To assess angiogenesis at the fascia-to-bone interface, CD31 (1:50; Abcam) was used. The sections were first deparaffinized in xylene and hydrated with a series of graded alcohol washes, and endogenous peroxidase was eliminated by 3% hydrogen peroxide. Later, the primary antibodies were incubated overnight at 4°C. After washing, the sections were incubated with a goat anti-rabbit immunoglobulin G secondary antibody to detect the primary

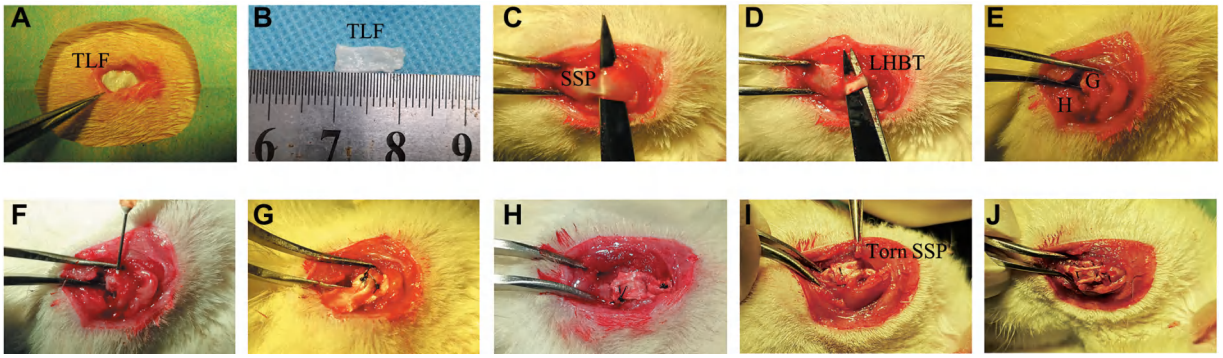


**Figure 2.** Surgical procedure. (A) Exposure of the thoracolumbar fascia (TLF). (B) Harvest graft of the TLF. (C) Visualization of the supraspinatus (SSP). (D) Visualization of the long head of the biceps tendon (LHBT). (E) Exposure of the humeral head (H) and glenoid (G). (F) Two holes were punched in the glenoid using needles. (G) One end of the TLF was fixed onto the glenoid. (H) The other side of the TLF was fixed onto the humerus. (I) Exposure of the torn SSP. (J) The remnant SSP was sutured into the medial part of the TLF.

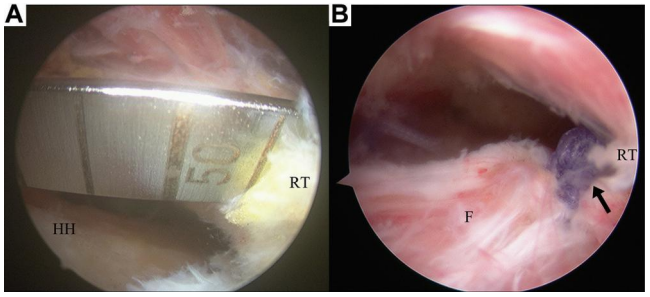


**Figure 3.** Arthroscopic views. (A) Massive rotator cuff tear. (B) The torn supraspinatus (SSP) was sutured onto the surface of the fascia lata graft with proper tension. The arrow indicates the fascia-to-tendon interface after suture and knotting. F, fascia lata; HH, humeral head; RT, remnant tendon of SSP.

antibodies. The sections were dehydrated, cleared, and coverslip put on the slide. After immunohistochemical staining, images were captured. The methods of evaluation have been described previously.[32]

## Clinical Study

The candidates for the procedures met the following inclusion criteria: (1) the torn rotator cuff tendon was diagnosed as an MRCT[15]; (2) the torn tendon could not be reconstructed on the footprint area under proper tension during arthroscopic surgery[38]; (3) the length of remnant SSP tendon was ≥5 mm for dSCR, and the length of remnant SSP tendon was <5 mm for SCR; (4) the Hamada grade was ≤3;[16] and (5) patients were followed for ≥1 year after surgery. The exclusion criteria included (1) subscapular tendon injury (Lafosse classification ≥2) and subscapular repair; (2) severe medical diseases, including angiocardiopathy and endocrine diseases; (3) cervical nerve palsy or axillary nerve palsy; (4) deltoid muscle dysfunction; and (5) history of infection in the glenohumeral joint.

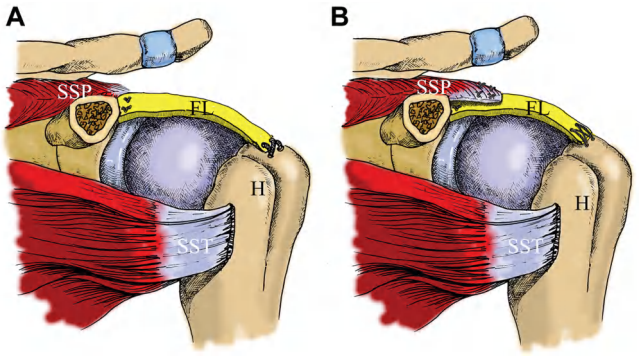


**Figure 4.** The surgical outlines of the different surgical methods. (A) Superior capsular reconstruction (SCR) group: the fascia lata (FL) is fixed on 1 side to the footprint of the humerus (H) and the other side is fixed to the superior glenoid. (B) Dynamic SCR group: the remnant of the supraspinatus (SSP) tendon is sutured to the medial part of the FL after the SCR procedure. SST, subscapular tendon.

### *Surgical Technique*

*dSCR Group.* The procedure was performed with the patient in the lateral decubitus position on the uninjured side and while the patient was under general anesthesia. The operative arm was placed at 30° of abduction, 20° of forward flexion, and natural rotation. A standard posterior portal was established, and then the arthroscope was placed into the glenohumeral joint. The conditions of the subscapularis, labrum, articular cartilage, and LHBT were evaluated and repaired through the anterior portal. Later, the degree of RCT and the acromial shape were evaluated, arthroscopic subacromial decompression was performed, and the anterior, posterior, and medial sides of the SSP stump were fully released. Tissue-grasping forceps were used to evaluate the repair tension of the SSP tendons. The extent of the torn SSP tendons was >5 cm (Figure 3A), and the torn SSP could not be fixed onto the footprint area.

Autologous FL was used for both the dSCR and SCR groups. The width of the FL was the length of the anterior and posterior rotator cuff defects measured under arthroscopy, and the graft length was twice the length of the internal and external defects. The FL was taken from the thigh and folded in the middle for later use. Then, 2 absorbable triple-loaded suture anchors were implanted above the glenoid (Gryphon; Mitek DePuy Synthes) and through the anterior and Neviaser portals, and the other 2 were implanted inside the greater tubercle. The sutures from the glenoid side anchor and inner row suture were sutured through the inner and outer ends of the graft, respectively, and then the graft was implanted through the lateral portal. The glenoid side and inner row suture were knotted, and 2 outer row anchors (Versalok; Mitek DePuy Synthes) were implanted.

The residual part of the SSP tendons was pulled outward and sutured onto the surface of the superior FL graft with proper tension, generally 4 stitches with 8-mm intervals (Figure 3B). Finally, a negative-pressure drainage vessel was used, and the incision was sutured layer by layer.

*SCR Group.* The procedure was completed according to the steps of dSCR; the difference was that the residual part of the SSP tendon was left untreated. The remnant of the infraspinatus (ISP) tendon was sutured to the posterior edge of the FL graft if the quality of the remnant of the ISP tendon could sustain the suture stretch. The final surgical outlines of the different surgical methods are shown in Figure 4.

#### *Postoperative Care and Follow-up*

Antibiotics were used for the first 24 hours postoperatively to prevent infection. The patients could move their wrist and elbow as soon as they came out of anesthesia. The drainage tube was removed 1 day after the operation, and the patient's arm was supported in an abduction sling for 6 weeks before limited and protected passive ROM was allowed. Active ROM and gentle strengthening were allowed at 6 weeks, and the injured shoulder could move normally without pain 3 months postoperatively.

All patients were followed up at 6 weeks and 3, 6, 9, and 12 months after surgery and then every 6 months to obtain functional and radiographic evaluations. The visual analog scale (VAS), American Shoulder and Elbow Surgeons (ASES), Constant, and University of California Los Angeles (UCLA) scores were used to evaluate the improvement in shoulder function, and the active ROM of the shoulder, including forward flexion, abduction, external rotation, and internal rotation, was recorded. And C1 to S5 are defined as numbers 1 to 29, respectively.[30] The changes in AHD were measured as the shortest distance between the dense cortical bone of the acromial inferior surface and the highest cortex of the humeral head in a standard anteroposterior radiograph as previously described.[14] In detail, all anteroposterior radiographs were taken by the same radiographer using the same positions and the same radiograph apparatus. Two authors (H.L. and Y.L.) measured AHD independently using computer-aided linear measurements (picture archiving and communication systems software, INFINITT; INFINITT Co). Fatty infiltration of the SSP muscle was also evaluated using the modified grading system of Goutallier based on MRI scan.[11,49] In detail, an oblique sagittal MRI fat analysis and calculation technique was used (a 1.5-T magnetic resonance scanner, Magnetom Essenza; Siemens) by 2 authors (H.L. and Y.L.).

### Statistical Analysis

All statistical analyses were performed using SPSS 22.0 software (IBM Corp). Data are presented as the mean ± SD. Statistical analyses of the modified tendon maturing score, semiquantitative cartilage areas, vessel numbers, shoulder function, and ROM between the 2 groups and AHD improvement were performed using independent-samples Student *t* tests. Preoperative and postoperative shoulder ROM and shoulder function improvement were assessed using a paired-samples *t* test. The Goutallier classification used the Mann-Whitney *U* nonparametric test. Differences of $P < .05$ were considered significant.

## RESULTS

### Animal Study

#### *Gross Evaluation*

TLFs were attached to the greater tuberosity in the 2 groups and healed with the remnant SSP tendons in the dSCR group, and no graft tears were found at any time point. The pale yellow color of TLFs, which reflects the inflammatory response in the SCR group, lasted until the fourth week after surgery. However, pale yellow in the fascia-to-bone and fascia-to-tendon interfaces was maintained for 2 weeks after surgery and turned light white 4 weeks after surgery in the dSCR group. The TLF tissue gradually migrated into the fibrous membranes and adhered to the anterior and posterior soft tissue 8 weeks after surgery in the SCR group and 4 weeks after surgery in the dSCR group (Figure 5).

#### *Histologic Evaluations*

The results of H&E staining showed that the structure of the TLF was intact, and the tissue of the fascia-to-bone interface was loose in both groups 1 week after TLF graft implantation. At 2 weeks after TLF graft implantation, numerous inflammatory cells were located at the fascia-to-bone junction in both groups. At 4 weeks after TLF graft implantation, the fascia-to-bone interface became dense, and the collagen fibers remained disorganized in both groups. At 8 weeks after TLF graft implantation, chondrocyte-like cells appeared at the fascia-to-bone junction, and the collagen fibers were oriented more regularly in the dSCR group. At 16 weeks after TLF graft implantation, 4 typical layers—tendon, unmineralized fibrocartilage, mineralized fibrocartilage, and bone—appeared in both groups (Figure 6). With regard to the modified tendon maturation score, the dSCR group had significantly higher

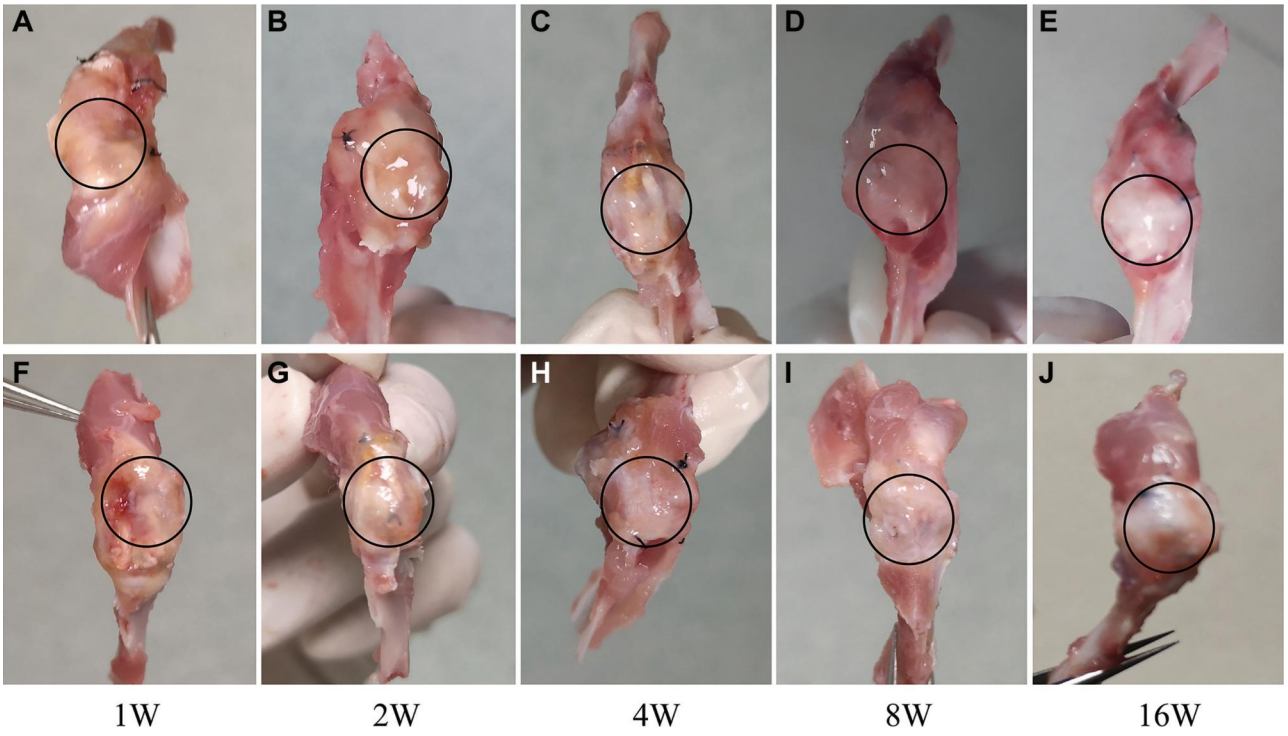


**Figure 5.** Macroscopic views of the (A-E) superior capsular reconstruction (SCR) and (F-J) dynamic SCR (dSCR) groups. The black circle shows the graft areas. The white fascial tissue gradually migrated into the fibrous membranes at 4 weeks postoperatively in the dSCR group and 8 weeks postoperatively in the SCR group.

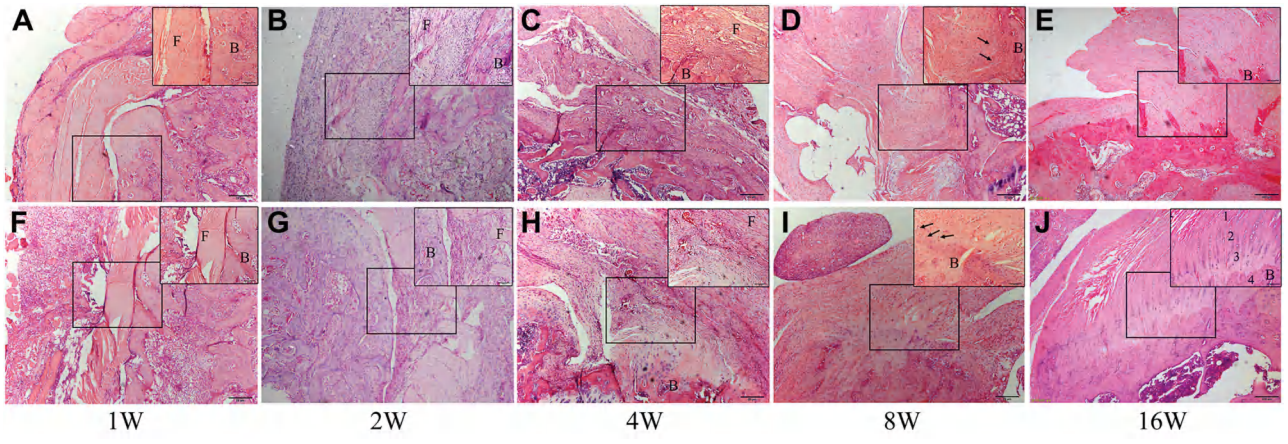


**Figure 6.** Hematoxylin and eosin staining at the fascia-to-bone interface of the (A-E) superior capsular reconstruction (SCR) and (F-J) dynamic SCR (dSCR) groups at 1, 2, 4, 8, and 16 weeks postoperatively. Chondrocyte-like cells (black arrows) appeared at the fascia-to-bone interface at 8 weeks in both groups. Four typical layers—tendon, unmineralized fibrocartilage, mineralized fibrocartilage, and bone (marked 1, 2, 3, and 4, respectively)—appeared in the dSCR group at 16 weeks. B, bone; F, fascia.

scores than the SCR group at 4, 8, and 16 weeks; the results are shown in Table 1.

After safranin O staining, the staining areas in the fascia-to-bone areas of both groups increased with the healing process. At 8 and 16 weeks, the extracellular matrices around the chondrocyte-like cells were stained with red safranin O in both groups, and the staining areas of the dSCR group were larger than those of the SCR group at 4, 8, and 16 weeks. A tidemark structure was observed in the dSCR group at 16 weeks (Figure 7J). Semiquantitative evaluation of the cartilage staining areas is shown in Table 2.

TABLE 1
Comparison of the Modified Tendon Maturation Scores Between the SCR and dSCR Groups[a]

| Time After Surgery (weeks) | dSCR Group | dSCR Group | *P* Value |
|---|---|---|---|
| 1 | 7.40 ± 0.55 | 7.60 ± 0.55 | .621 |
| 2 | 9.20 ± 0.84 | 10.20 ± 1.30 | .089 |
| 4 | 12.20 ± 1.30 | 14.60 ± 1.52 | **.004** |
| 8 | 19.60 ± 1.14 | 22.20 ± 1.10 | **.019** |
| 16 | 23.80 ± 0.84 | 26.20 ± 0.84 | **.024** |

[a]Values are presented as weeks after surgery or mean ± SD; Bold values indicate statistical significance. dSCR, dynamic superior capsular reconstruction; SCR, superior capsular reconstruction.

TABLE 2
Semiquantitative Evaluation of the Cartilage Staining Areas Between the SCR and dSCR Groups[a]

| Time After Surgery (wk) | SCR Group (%) | dSCR Group (%) | *P* Value |
|---|---|---|---|
| 1 | — | — | — |
| 2 | — | — | — |
| 4 | 0.770 ± 0.153 | 1.032 ± 0.104 | **.028** |
| 8 | 16.216 ± 1.681 | 29.118 ± 2.916 | **.002** |
| 16 | 45.838 ± 2.965 | 51.618 ± 2.756 | **.037** |

[a]Values are presented as weeks after surgery or mean ± SD; Bold values indicate statistical significance; The dashes indicate that no cartilage staining was detected; dSCR, dynamic superior capsular reconstruction; SCR, superior capsular reconstruction.

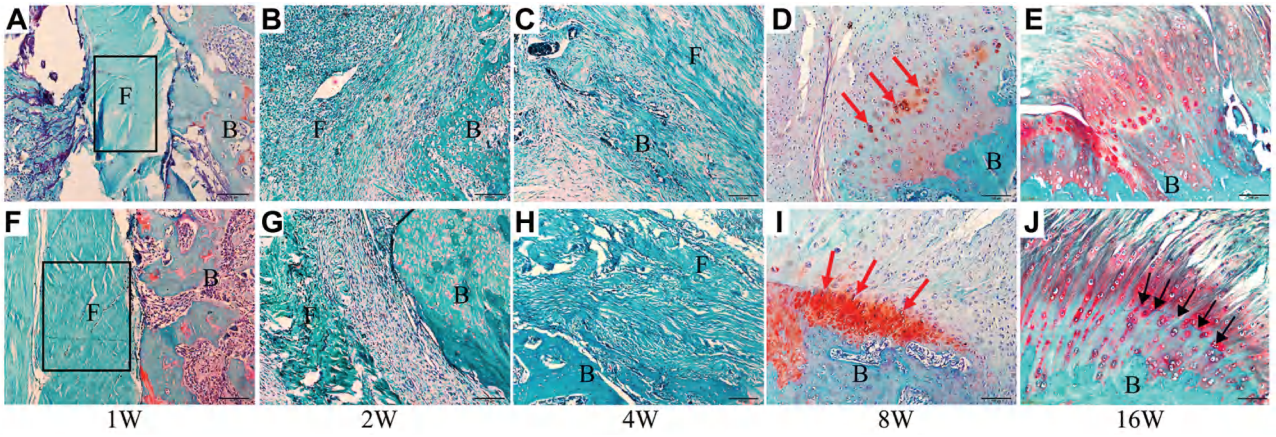


**Figure 7.** Safranin O staining of the fascia-to-bone interface in the (A-E) superior capsular reconstruction (SCR) and (F-J) dynamic SCR (dSCR) groups at 1, 2, 4, 8, and 16 weeks after thoracolumbar fascial (TLF) graft implantation postoperatively. The TLF (rectangle) was measured at 1 week in both groups, chondrocyte-like cells (red arrows) were observed in both groups at 8 weeks, and tidemarks (black arrows) were observed at 16 weeks in the dSCR group. B, bone; F. fascia.

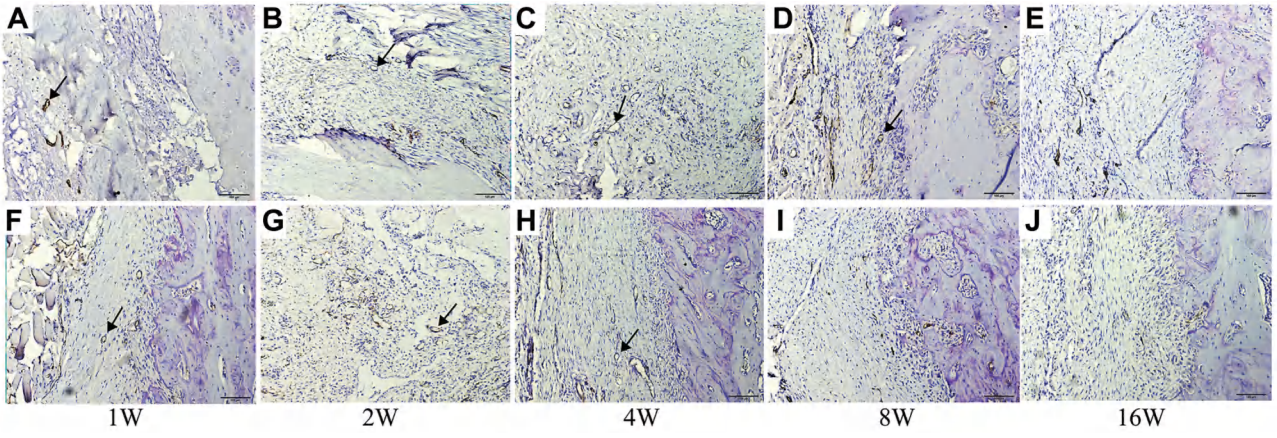


**Figure 8.** Immunohistochemistry using an endothelium-specific anti-CD31 antibody showed the ingrowth of blood vessels in the (A-E) superior capsular reconstruction (SCR) and (F-J) dynamic SCR groups. The black arrow indicates the vessel.

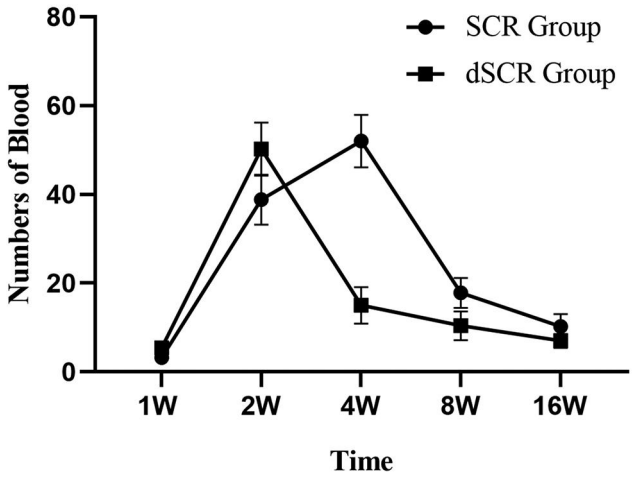


**Figure 9.** Angiogenesis in the fascia-to-bone junction peaked at 2 weeks (W) preoperatively in the dynamic superior capsular reconstruction (dSCR) group and at 4 weeks postoperatively in the superior capsular reconstruction (SCR) group, with stable conditions after 2 and 4 weeks of thoracolumbar fascial graft implantation in the dSCR group and 4 and 8 weeks in the SCR group, respectively.

### *Immunohistochemical Evaluations*

The fascia-to-bone interface began to revascularize 1 week postoperatively (Figure 8). The peak of angiogenesis in the dSCR group occurred earlier and decreased faster than that in the SCR group (Figure 9). At 16 weeks after TLF graft implantation, little angiogenesis was detected in either group.

## Clinical Study

### *Clinical Results*

All 22 patients completed a minimum of 12 months of follow-up after surgery, and no patients dropped out. No significant differences were detected between the 2 groups in terms of age, course of disease, defect length from medial to lateral, defect length from anterior to posterior, or follow-up time (Table 3). Two patients in the conventional SCR group and none in the dSCR group accepted suturing of the ISP tendon to the posterior edge of the FL graft. During the follow-up, 2 postoperative complications were found in the SCR group: 1 case of wound infection and 1 case of graft retear.

ROM, including forward flexion, abduction, external rotation, and internal rotation, and functional scores, including the mean VAS score, the ASES score, and the UCLA score, were significantly improved at the last follow-up compared with the preoperative values for both the conventional SCR group (Table 4) and the dSCR group (Table 5). The degree of improvement, including active ROM, VAS, Constant scores, and AHD, in the dSCR group was significantly higher than that in the conventional SCR group. However, there was no significant difference in forward flexion and UCLA and ASES scores (Table 6).

TABLE 3
General Characteristics of the Patients in the SCR and dSCR Groups[a]

| | SCR | dSCR | P value |
|---|---|---|---|
| No. | 9 | 13 | |
| Male | 2 | 6 | |
| Female | 7 | 7 | |
| Age, y | 61.22 ± 6.81 | 65.54 ± 8.39 | .217 |
| Duration of course, mo | 30.44 ± 35.56 | 29.15 ± 20.94 | .407 |
| Follow up time, mo | 22.89 ± 7.59 | 25.62 ± 7.32 | .916 |
| Defect length, cm | | | |
| Medial-lateral | 5.83 ± 0.79 | 5.35 ± 0.47 | .124 |
| Anterior-posterior | 3.89 ± 0.65 | 3.81 ± 0.60 | .765 |

[a]Data are presented as number of patients or mean ± SD.

TABLE 4
Comparison of the Active ROM, Shoulder Function Scores, and AHD in Patients With SCR Preoperatively and at the Last Follow-up[a]

| | Preoperatively | Last follow-up | P value |
|---|---|---|---|
| Active ROM | | | |
| FF, deg | 90.56 ± 29.20 | 147.78 ± 10.93 | **<.001** |
| Abduction, deg | 87.78 ± 27.74 | 144.44 ± 8.82 | **<.001** |
| ER, deg | 22.78 ± 8.70 | 47.78 ± 6.67 | **.009** |
| IR, grade | 23.56 ± 1.59 | 20.78 ± 1.20 | **<.001** |
| Shoulder Function Score | | | |
| VAS | 4.22 ± 0.83 | 1.22 ± 0.83 | **<.001** |
| ASES | 42.41 ± 13.56 | 86.48 ± 5.69 | **<.001** |
| UCLA | 12.89 ± 3.02 | 28.89 ± 2.42 | **<.001** |
| Constant | 35.22 ± 10.37 | 83.11 ± 7.96 | **<.001** |
| Acromiohomeral distance | 3.17 ± 1.61 | 9.23 ± 1.48 | **<.001** |

[a]Values are presented as mean ± SD; Bold values indicate statistical significance. ASES, American Shoulder and Elbow Surgeons; ER, external rotation; FF, forward flexion; IR, internal rotation cone rank; ROM, range of motion; SCR, superior capsular reconstruction; UCLA, University of California Los Angeles; VAS, visual analog scale.

The degree of improvement in AHD at the last follow-up showed that there was significant improvement compared with the preoperative AHD in both the conventional SCR and the dSCR groups. Moreover, the degree of improvement in AHD in the dSCR group was significantly higher than that in the conventional SCR group (Table 6). Fatty infiltration at the last follow-up was significantly improved compared with that preoperatively in both the conventional SCR and the dSCR groups. However, there were no significant differences between the 2 groups, as shown in Table 7. Radiographs of a typical dSCR case are shown in Figure 10.

## DISCUSSION

SCR has been increasingly frequently used as a joint-preserving treatment for IMRCT.[21,43] Conventional SCR

TABLE 5
Comparison of the Active ROM, Shoulder Function Scores, and AHD in the Patients With dSCR Preoperatively and at the Last Follow-up[a]

| | Preoperatively | Last follow-up | P value |
|---|---|---|---|
| Active ROM | | | |
| FF, deg | 76.54 ± 34.12 | 157.69 ± 8.32 | **<.001** |
| Abduction, deg | 70.38 ± 33.32 | 156.92 ± 13.77 | **<.001** |
| ER, deg | 20.77 ± 7.03 | 53.85 ± 4.63 | **<.001** |
| IR, grade | 24.00 ± 0.91 | 19.62 ± 1.33 | **<.001** |
| Shoulder Function Score | | | |
| VAS | 4.54 ± 0.78 | 0.52 ± 0.65 | **<.001** |
| ASES | 42.68 ± 8.72 | 92.72 ± 4.59 | **<.001** |
| UCLA | 12.62 ± 3.07 | 31.08 ± 1.98 | **<.001** |
| Constant | 31.15 ± 10.02 | 90.31 ± 6.41 | **<.001** |
| Acromiohomeral distance | 5.70 ± 1.72 | 10.08 ± 1.46 | **<.001** |

[a]Values are presented as mean ± SD; Bold values indicate statistical significance. ASES, American Shoulder and Elbow Surgeons; dSCR, dynamic superior capsular reconstruction; ER, external rotation; FF, forward flexion; IR, internal rotation cone rank; ROM, range of motion; UCLA, University of California Los Angeles; VAS, visual analog scale.

TABLE 6
Comparison of the Degree of Improvement in the Active ROM, Shoulder Function Scores, and AHD Between the SCR and dSCR Groups Preoperatively and at the Last Follow-up[a]

| | SCR | dSCR | P value |
|---|---|---|---|
| Active ROM | | | |
| FF, deg | 57.22 ± 24.89 | 81.15 ± 33.05 | .081 |
| Abduction, deg | 56.67 ± 27.39 | 86.54 ± 30.37 | **.029** |
| ER, deg | 25.00 ± 9.35 | 33.08 ± 8.55 | **.049** |
| IR, grade | −2.78 ± 2.44 | −4.38 ± 1.12 | **.049** |
| Shoulder Function Score | | | |
| VAS | −3.00 ± 0.87 | −3.92 ± 0.95 | **.031** |
| ASES | 44.07 ± 15.44 | 50.03 ± 7.85 | .246 |
| UCLA | 16.00 ± 4.50 | 18.46 ± 3.45 | .162 |
| Constant | 47.89 ± 15.39 | 59.15 ± 9.74 | **.048** |
| Acromiohomeral distance | 3.06 ± 1.41 | 4.38 ± 1.35 | **.039** |

[a]Values are presented as mean ± SD; Bold values indicate statistical significance. ASES, American Shoulder and Elbow Surgeons; dSCR, dynamic superior capsular reconstruction; ER, external rotation; FF, forward flexion; IR, internal rotation cone rank; ROM, range of motion; SCR, superior capsular reconstruction; UCLA, University of California Los Angeles; VAS, visual analog scale.

does not restore the dynamic effects of the SSP tendon. dSCR has been tried as a method to restore the dynamic effects of the SSP tendon by suturing the remnant of the SSP tendon to the medial part of the FL graft after SCR. In this study, we investigated the effect of dSCR on fascia-to-bone healing and evaluated the short-term clinical effect of dSCR.

SCR effectively restores the stability of the shoulder joint and improves the clinical function of patients with IMRCT.[1,28,31,37,46] The conventional SCR not only connects the footprint of the greater tubercle and superior glenoid using a graft but also includes side-to-side suture of the residual infraspinatus tendon and anterior SSP tendon to the FL graft.[5,54] Posterior side-to-side suturing between the graft and the ISP tendons showed better shoulder stability according to the cadaveric biomechanical test.[41] It is important to ensure capsular continuity to restore superior stability and dynamics to a certain degree after surgery.[34] However, conventional SCR does not include suture of the medial remnant of the SSP tendon. dSCR could transmit the contractile force of the SSP to the graft and the humerus by suturing the remnant SSP tendon to the FL autograft. In this study, there were only 2 cases in the conventional SCR group that underwent suture repair of the ISP tendon because of reparable quality. In view of improving clinical outcome, we have reason to believe that repairing the ISP is a minor factor for the clinical outcome compared with SCR itself. A cadaveric biomechanical test and living animal research are needed to define the effect of suturing the ISP tendon and/or remnant SSP tendon in the future. In other words, dSCR theoretically has more dynamic potential in the shoulder.

The FL graft can regenerate the fibrocartilaginous insertion in rabbit and rat SCR models.[19,32] Compared with the SCR group, the rats in the dSCR group showed a higher maturity of histologic structure across the fascia-to-bone interface, and chondrocyte-like cells appeared earlier. Additionally, angiogenesis reached peak values and stable conditions in the dSCR group earlier than in the SCR group. Mechanically stimulated constructs induced cell orientation and an effectively aligned collagen and tenomodulin extracellular matrix.[10] The fascia-to-bone healing in the dSCR group was better than that in the SCR group. The possible reason was that dSCR restored the dynamics of the torn SSP tendon. In summary, suitable muscle contractile force might promote fascia-to-bone healing.

Both the dSCR and SCR groups achieved significant improvement in the active ROM and shoulder function scores at the last follow-up. Additionally, the results of the ROM, VAS, and shoulder function scores were significantly improved in the dSCR group compared with the SCR group. These clinical results were consistent with the histologic findings of fascia-to-bone healing. The fascia-to-bone interface in the dSCR group healed faster, and its tissue density was higher. In the early process of postoperative healing, a large number of blood vessels were generated in the dSCR group, which was conducive to the growth of tissues. In the process of fascial transition to tendon-like tissue, the number of blood vessels gradually decreased, and the rate of decline in the dSCR group was faster. The decrease in the number of blood vessels in the late healing process indicates that the histologic structure was maturing. Healing of the muscle-tendon-bone unit is load intensity dependent.[23,53] Mechanical properties cause nano- and microscale observations at the tissue level.[25,48] Therefore, strain from the SSP muscle after dSCR might cause angiogenesis changes. These changes might cause differences in fascia-to-bone healing and clinical outcomes between the dSCR group and SCR group.

TABLE 7
Comparison of Fat Infiltration Between the SCR and dSCR Groups Preoperatively and at the Last Follow-up[a]

| | | Goutallier Classification | | | | | | | | |
|---|---|---|---|---|---|---|---|---|---|---|
| | | Preoperatively | | | | LFP | | | | |
| Group | No. of Patients | 1 | 2 | 3 | 4 | 1 | 2 | 3 | 4 | *P* Value |
| SCR | 9 | 0 | 5 | 3 | 1 | 3 | 5 | 1 | 0 | **.036** |
| dSCR | 13 | 0 | 4 | 4 | 5 | 7 | 4 | 2 | 0 | **.001** |
| *P* Value | — | .155 | | | | .511 | | | | — |

[a]Datas are presented as number of patients or Goutalliar grade. Bold values indicate statistical significance. dSCR, dynamic superior capsular reconstruction; LFP, last follow-up; SCR, superior capsular reconstruction.

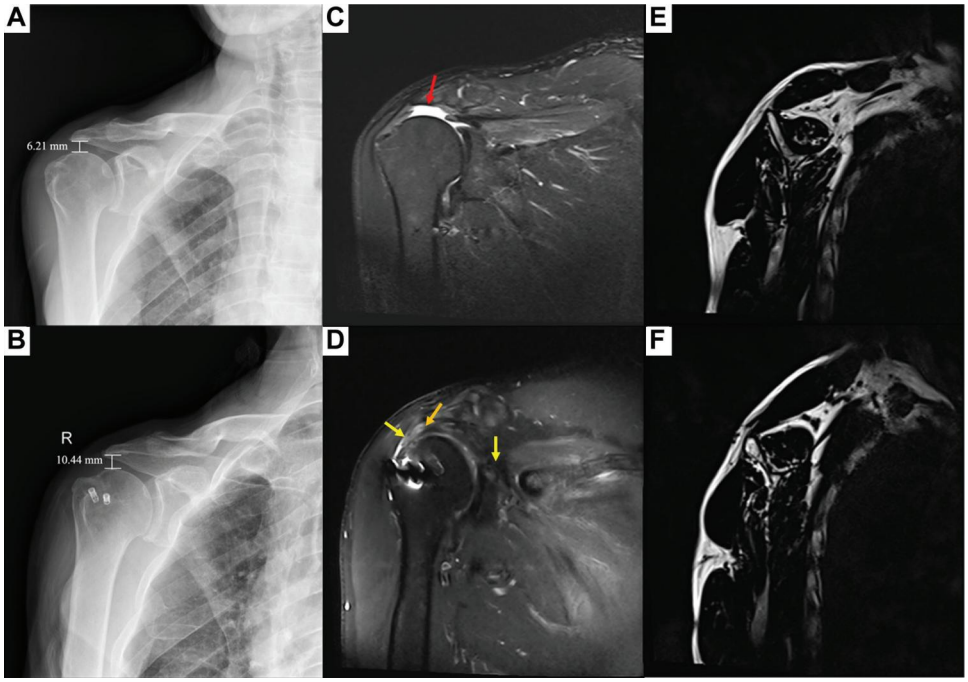


**Figure 10.** (A) Preoperative radiograph obtained in a 66-year-old man showing a narrow acromiohumeral distance (AHD). (B) Postoperative 24-month radiograph showing that the AHD had increased from 6.21 mm to 10.44 mm. (C) Preoperative coronal magnetic resonance imaging (MRI) scan showing massive rotator cuff tear (arrow). (D) Postoperative 24-month coronal MRI scan showing well-incorporated fascia lata to the greater tuberosity (The yellow arrows refer to the medial and lateral endings of the fascia lata graft, and the orange arrow refers to the middle part of the fascia lata graft) and superior glenoid. (E) Oblique sagittal preoperative coronal MRI scan showing a large area of fat infiltration in the supraspinatus (SSP) muscle; the Goutallier classification is 3. (F) Postoperative 24-month oblique sagittal MRI scan showing little infiltration in the SSP; the Goutallier classification is 1.

The bridging patch technique could also restore the dynamics of the SSP, and this technique includes directly suturing the graft and the remnant tendon in a side-to-side style.[47] When the quality of the remaining muscle and tendon is poor, the bridging patch technique runs a great risk of retear in the graft-tendon interface. In fact, it is difficult to restore the length-tension relation without overtension for the bridging patch technique.[47] However, dSCR could minimize the retear risk when SCR affords stability compared with the bridging patch technique.[2] Xu et al[55] introduced dual-suspensory reconstruction using banded grafts, which increased the biomechanical strength when compared with the routine patch technique. Together, dSCR could achieve a good clinical outcome, and the indication for dSCR was good quality of the remnant SSP tendon and muscle.

Radiographic results showed that both AHD and fatty infiltration achieved significant improvement postoperatively. However, at the last follow-up, only the degree of improvement in AHD showed a significant difference in the dSCR group. IMRCTs result in excessive upward movement of the humeral head because of loss of superior

stability.[9] The in vivo dynamic minimum AHD was 0.9 mm in RCT shoulders and 2.1 mm in healthy shoulders at 90° of arm abduction.[42] In this study, arthroscopic acromial decompression was performed for every patient, which aimed to decrease the possibility of subacromial impingement and increase graft survival. At the last follow-up, the degree of AHD improvement in the dSCR group was significantly improved compared with that in the SCR group. On one hand, it indicated that superior stability was restored; on the other hand, stretch in the fascia-to-tendon interface, which came from the SSP, might cause a higher AHD in the dSCR group. The severity of fatty infiltration in the SSP muscle preoperatively is associated with a higher retear rate and was considered a predictor of poor shoulder function.[12,13,17] In this study, fatty infiltration in the SSP muscle was significantly improved in both groups postoperatively. These results were consistent with Hamano et al's[17] report that fatty infiltration improved significantly at 1 year after successful rotator cuff repair. However, there was no significant difference in fatty infiltration between the 2 groups. The effect of continuous mechanical traction on the SSP muscle in the dSCR theoretically inhibits the formation of fat in the SSP muscle, and longer follow-up might be needed. Together, both dSCR and conventional SCR achieved improvements in AHD and fatty infiltration.

This study has several limitations. First, we did not quantify the dynamic effect of SSP, which comes from the fascia-to-tendon interface, and use of an isokinetic dynamometer with an isokinetic shoulder strength test might distinguish tiny changes. Second, only 22 patients were included in this study, and the mean follow-up time was 22 months. However, we aimed to investigate the effect of dSCR on fascia-to-bone healing and the short-term clinical effectiveness of dSCR in patients with IMRCT. A controlled laboratory study as the preclinical study and a cohort clinical study between dSCR and conventional SCR are appropriate. Additionally, the histologic and clinical data were robust. Therefore, the limitation does not weaken the conclusion. Further research is needed to discover the molecular mechanism of dSCR on fascia-to-tendon healing and quantify the dynamic effect of dSCR.

## CONCLUSION

dSCR promoted faster fascia-to-bone healing in a rat model and provided superior clinical results at short term compared with conventional SCR.

## REFERENCES


1. Berthold DP, Muench LN, Dyrna F, et al. Comparison of different fixation techniques of the long head of the biceps tendon in superior capsule reconstruction for irreparable posterosuperior rotator cuff tears: a dynamic biomechanical evaluation. *Am J Sports Med*. 2021;49(2):305-313.
2. Bi M, Zhou K, Gan K, et al. Combining fascia lata autograft bridging repair with artificial ligament internal brace reinforcement: a novel healing-improvement technique for irreparable massive rotator cuff tears. *Bone Joint J*. 2021;103(10):1619-1626.
3. Cabarcas BC, Garcia GH, Gowd AK, Liu JN, Romeo AA. Arthroscopic superior capsular reconstruction and over-the-top rotator cuff repair incorporation for treatment of massive rotator cuff tears. *Arthrosc Tech*. 2018;7(8):e829-e837.
4. Christian RA, Stabile KJ, Gupta AK, et al. Histologic analysis of porcine dermal graft augmentation in treatment of rotator cuff tears. *Am J Sports Med*. 2021;49(13):3680-3686.
5. Cohn MR, Amar S, Garrigues GE, Verma NN. Superior capsular reconstruction: proposed biomechanical advantages. *Arthroscopy*. 2022;38(1):20-21.
6. Daisuke M, Kazuha K, Noboru F, et al. Irreparable large to massive rotator cuff tears with low-grade fatty degeneration of the infraspinatus tendon: minimum 7-year follow-up of fascia autograft patch procedure and partial repair. *Am J Sports Med*. 2021;49(13):3656-3668.
7. Denard PJ, Brady PC, Adams CR, Tokish JM, Burkhart SS. Preliminary results of arthroscopic superior capsule reconstruction with dermal allograft. *Arthroscopy*. 2018;34(1):93-99.
8. Fandridis E, Zampeli F. Superior capsular reconstruction with double bundle of long head biceps tendon autograft: the ''box'' technique. *Arthrosc Tech*. 2020;9(11):e1747-e1757.
9. Franceschi F, Papalia R, Vasta S, et al. Surgical management of irreparable rotator cuff tears. *Knee Surg Sports Traumatol Arthrosc*. 2015;23(2):494-501.
10. Garcia Garcia A, Perot JB, Beldjilali-Labro M, et al. Monitoring mechanical stimulation for optimal tendon tissue engineering: a mechanical and biological multiscale study. *J Biomed Mater Res A*. 2021;109(10):1881-1892.
11. Goutallier D, Postel JM, Bernageau J, Lavau L, Voisin MC. Fatty muscle degeneration in cuff ruptures. Pre- and postoperative evaluation by CT scan. *Clin Orthop Relat Res*. 1994;304:78-83.
12. Goutallier D, Postel JM, Gleyze P, Leguilloux P, Van Driessche S. Influence of cuff muscle fatty degeneration on anatomic and functional outcomes after simple suture of full-thickness tears. *J Shoulder Elbow Surg*. 2003;12(6):550-554.
13. Goutallier D, Postel JM, Radier C, Bernageau J, Zilber S. Long-term functional and structural outcome in patients with intact repairs 1 year after open transosseous rotator cuff repair. *J Shoulder Elbow Surg*. 2009;18(4):521-528.
14. Gruber G, Bernhardt GA, Clar H, et al. Measurement of the acromiohumeral interval on standardized anteroposterior radiographs: a prospective study of observer variability. *J Shoulder Elbow Surg*. 2010;19(1):10-13.
15. Habermeyer P, Krieter C, Tang KL, Lichtenberg S, Magosh P. A new arthroscopic classification of articular-sided supraspinatus footprint lesions: a prospective comparison with Snyder's and Ellman's classification. *J Shoulder Elbow Surg*. 2008;17(6):909-913.
16. Hamada K, Fukuda H, Mikasa M, Kobayashi Y. Roentgenographic findings in massive rotator cuff tears. A long-term observation. *Clin Orthop Relat Res*. 1990;254:92-96.
17. Hamano N, Yamamoto A, Shitara H, et al. Does successful rotator cuff repair improve muscle atrophy and fatty infiltration of the rotator cuff? A retrospective magnetic resonance imaging study performed shortly after surgery as a reference. *J Shoulder Elbow Surg*. 2017;26(6):967-974.
18. Harada Y, Mifune Y, Inui A, et al. Rotator cuff repair using cell sheets derived from human rotator cuff in a rat model. *J Orthop Res*. 2016;35(2):289-296.
19. Hasegawa A, Mihata T, Itami Y, Fukunishi K, Neo M. Histologic changes during healing with autologous fascia lata graft after superior capsule reconstruction in rabbit model. *J Shoulder Elbow Surg*. 2021;30(10):2247-2259.
20. Ide J, Kikukawa K, Hirose J, et al. Reconstruction of large rotator-cuff tears with acellular dermal matrix grafts in rats. *J Shoulder Elbow Surg*. 2009;18(2):288-295.
21. Ishihara Y, Mihata T, Tamboli M, et al. Role of the superior shoulder capsule in passive stability of the glenohumeral joint. *J Shoulder Elbow Surg*. 2014;23(5):642-648.

22. Jones CR, Snyder SJ. Massive irreparable rotator cuff tears: a solution that bridges the gap. *Sports Med Arthrosc Rev*. 2015;23(3):130-138.
23. Killian ML, Cavinatto L, Galatz LM, Thomopoulos S. The role of mechanobiology in tendon healing. *J Shoulder Elbow Surg*. 2012;21(2):228-237.
24. Killian ML, Cavinatto LM, Ward SR, Havlioglu N, Galatz LM. Chronic degeneration leads to poor healing of repaired massive rotator cuff tears in rats. *Am J Sports Med*. 2015;43(10):2401-2410.
25. Kim D, Lee B, Marshall B, Thomopoulos S, Jun YS. Cyclic strain enhances the early stage mineral nucleation and the modulus of demineralized bone matrix. *Biomater Sci*. 2021;9(17):5907-5916.
26. Kim YS, Lee HJ, Park I, et al. Arthroscopic in situ superior capsular reconstruction using the long head of the biceps tendon. *Arthrosc Tech*. 2018;7(2):e97-e103.
27. Kovacevic D, Suriani RJ Jr, Levine WN, Thomopoulos S. Augmentation of rotator cuff healing with orthobiologics. *J Am Acad Orthop Surg*. 2022;30(5):e508-e516.
28. Lacheta L, Brady A, Rosenberg SI, et al. Superior capsule reconstruction with a 3 mm–thick dermal allograft partially restores glenohumeral stability in massive posterosuperior rotator cuff deficiency: a dynamic robotic shoulder model. *Am J Sports Med*. 2021;49(8):2056-2063.
29. Li H, Zhou B, Tang K. Advancement in arthroscopic superior capsular reconstruction for irreparable massive rotator cuff tear. *Orthop Surg*. 2021;13(7):1951-1959.
30. Li HS, Ma L, Li Y, et al. The short-term effectiveness of superior capsular reconstruction using autologous fascia lata graft for irreparable massive rotator cuff tears. *J Chin Rep Recons Surg*. 2021;35(11):1427-1433.
31. Li HS, Yang MY, Li Y, Zhou BH. Research progress of indication and treatment of graft in shoulder superior capsular reconstruction for rotator cuff tear. *J Chin Rep Recons Surg*. 2021;35(2):252-257.
32. Li HS, Zhou M, Huang P, et al. Histologic and biomechanical evaluation of the thoracolumbar fascia graft for massive rotator cuff tears in a rat model. *J Shoulder Elbow Surg*. 2022;31(4):699-710.
33. Liao YT, Li HS, Li Y, et al. Revascularization character of autologous fascia lata graft following shoulder superior capsule reconstruction by enhanced magnetic resonance imaging. *J Orthop Surg Res*. 2022;17(1):485.
34. Liao YT, Zhou BH, Mihata T. Superior capsule reconstruction: anatomy, biomechanics, indications, and graft treatment. *Chin Med J*. 2021;134(23):2847-2849.
35. MacDonald P, Verhulst F, McRae S, et al. Biceps tenodesis versus tenotomy in the treatment of lesions of the long head of the biceps tendon in patients undergoing arthroscopic shoulder surgery: a prospective double-blinded randomized controlled trial. *Am J Sports Med*. 2020;48(6):1439-1449.
36. Merolla G, Chillemi C, Franceschini V, et al. Tendon transfer for irreparable rotator cuff tears: indications and surgical rationale. *Muscles Ligaments Tendon J*. 2015;4(4):425-432.
37. Mihata T, Lee TQ, Fukunishi K, et al. Return to sports and physical work after arthroscopic superior capsule reconstruction among patients with irreparable rotator cuff tears. *Am J Sports Med*. 2018;46(5):1077-1083.
38. Mihata T, Lee TQ, Hasegawa A, et al. Arthroscopic superior capsule reconstruction for irreparable rotator cuff tears: comparison of clinical outcomes with and without subscapularis tear. *Am J Sports Med*. 2020;48(14):3429-3438.
39. Mihata T, Lee TQ, Hasegawa A, et al. Five-year follow-up of arthroscopic superior capsule reconstruction for irreparable rotator cuff tears. *J Bone Joint Surg Am*. 2019;101(21):1921-1930.
40. Mihata T, Lee TQ, Watanabe C, et al. Clinical results of arthroscopic superior capsule reconstruction for irreparable rotator cuff tears. *Arthroscopy*. 2013;29(3):459-470.
41. Mihata T, McGarry MH, Kahn T, Goldberg I, Neo M, Lee TQ. Biomechanical role of capsular continuity in superior capsule reconstruction for irreparable tears of the supraspinatus tendon. *Am J Sports Med*. 2016;44(6):1423-1430.
42. Naoya K, Takamitsu O, Naohide T, et al. In vivo dynamic acromiohumeral distance in shoulders with rotator cuff tears. *Clin Biomech*. 2018;60:95-99.
43. Nimura A, Kato A, Yamaguchi K, et al. The superior capsule of the shoulder joint complements the insertion of the rotator cuff. *J Shoulder Elbow Surg*. 2012;21(7):867-872.
44. Novi M, Kumar A, Paladini P, Porcellini G, Merolla G. Irreparable rotator cuff tears: challenges and solutions. *Orthop Res Rev*. 2018;10:93-103.
45. Patel S, Caldwell JM, Doty SB, et al. Integrating soft and hard tissues via interface tissue engineering. *J Orthop Res*. 2018;36(4):1069-1077.
46. Pauzenberger L, Heuberer PR, Dyrna F, et al. Double-layer rotator cuff repair: anatomic reconstruction of the superior capsule and rotator cuff improves biomechanical properties in repairs of delaminated rotator cuff tears. *Am J Sports Med*. 2018;46(13):3165-3173.
47. Rhee SM, Oh JH. Bridging graft in irreparable massive rotator cuff tears: autogenic biceps graft versus allogenic dermal patch graft. *Clin Orthop Surg*. 2017;9(4):497-505.
48. Richardson WJ, Kegerreis B, Thomopoulos S, Holmes JW. Potential strain-dependent mechanisms defining matrix alignment in healing tendons. *Biomech Model Mechanobiol*. 2018;17(6):1569-1580.
49. Rulewicz GJ, Beaty S, Hawkins RJ, Kissenberth MJ. Supraspinatus atrophy as a predictor of rotator cuff tear size: an MRI study utilizing the tangent sign. *J Shoulder Elbow Surg*. 2013;22(6):e6-e10.
50. Sevivas N, Ferreira N, Andrade R, et al. Reverse shoulder arthroplasty for irreparable massive rotator cuff tears: a systematic review with meta-analysis and meta-regression. *J Shoulder Elbow Surg*. 2017;26(9):e265-e277.
51. Shepet KH, Liechti DJ, Kuhn JE. Nonoperative treatment of chronic, massive irreparable rotator cuff tears: a systematic review with synthesis of a standardized rehabilitation protocol. *J Shoulder Elbow Surg*. 2021;30(6):1431-1444.
52. Stoll LE, Codding JL. Lower trapezius tendon transfer for massive irreparable rotator cuff tears. *Orthop Clin North Am*. 2019;50(3):375-382.
53. Thomopoulos S, Zampiakis E, Das R, Silva MJ, Gelberman RH. The effect of muscle loading on flexor tendon-to-bone healing in a canine model. *J Orthop Res*. 2008;26(12):1611-1617.
54. Vredenburgh ZD, Prodromo JP, Tibone JE, et al. Biomechanics of tensor fascia lata allograft for superior capsule reconstruction. *J Shoulder Elbow Surg*. 2021;30(1):178-187.
55. Xu J, Han K, Ye Z, et al. Biomechanical and histological results of dual-suspensory reconstruction using banded tendon graft to bridge massive rotator cuff tears in a chronic rabbit model. *Am J Sports Med*. 2022;50(10):2767-2781.
56. Yang F, Richardson DW. Comparative analysis of tenogenic gene expression in tenocyte-derived induced pluripotent stem cells and bone marrow-derived mesenchymal stem cells in response to biochemical and biomechanical stimuli. *Stem Cells Int*. 2021;2021:8835576.